2011

Thermally, Photochemically and Electrically Switchable Reflection Colors From Self-Organized Chiral Bent-Core Liquid Crystals

Quan Li, *Kent State University - Kent Campus*
Manoj Mathews
Rafael S. Zola
Deng-ke Yang

Thermally, photochemically and electrically switchable reflection colors from self-organized chiral bent-core liquid crystals

Manoj Mathews, Rafael S. Zola, Deng-ke Yang and Quan Li*

Received 15th October 2010, Accepted 3rd November 2010
DOI: 10.1039/c0jm03479g

We report the synthesis and characterization of two new chiral 1,3-phenylene based five ring bent-core mesogens that combine the unique electro-optic characteristics of banana-shaped molecules with chiroptic properties. Azobenzene moiety incorporated as a linking unit in one of the rigid arms renders *trans–cis* isomerization property to the molecules while chirality is introduced by tethering chiral aliphatic terminal chains. Both compounds can self-organize into helical superstructure, *i.e.* cholesteric mesophase, which can selectively reflect light. The novelty of the helical self-organized superstructure reported here lies in its low molecular weight single component molecular system that is truly multifunctional so that the reflection band is tunable by three different external stimuli, *i.e.* temperature, light and electric field. A red shift in reflection colors is obtained by changing the temperature on cooling and by UV irradiation while a blue shift is seen by electrical field application. Due to the high applicability of azobenzene-doped liquid crystalline systems, we also evaluated the efficiency of these chiral bent-core molecules as chiral transfer agents and found that they behave similar to rod-shaped dopants whose chirality is a consequence of the presence of one chiral center.

Introduction

The interplay between molecular structure and chirality has proved extremely fascinating for the design of various functional molecular assemblies.[1] Intensive work has focused on chiral liquid crystal (LC) molecules which self-organize into various technologically important mesophase structures such as cholesteric (N*), ferroelectric/antiferroelectric smectic phases and blue phases.[2] In most cases, the chiral phases are obtained by tethering chiral units covalently to the conventional rod-, disc-shaped or polymeric mesogenic molecules. Alternatively, a chiral dopant dissolved in an achiral LC phase can also induce chiral mesophases.[3] A notable exception is seen in mesophases of achiral bent-core (banana-shaped) LCs where the steric packing of molecules leads to polar order and chiral conformational states though the molecules are achiral.[4] Most often spontaneous symmetry breaking leads to racemic mixture of both (+) and (−) chiral conformers.[5] However, enantiomeric excess can be induced by external stimuli such as electric field,[6] chiral surfaces,[7] chiral dopants[8] and circularly polarized light[9] to obtain chirality related properties, *i.e.* ferroelectric and antiferroelectric switching,[4–6] large optical rotation[10] and chiral non-linear optic effects.[11]

Although a large number of structurally different bent-core mesogens have been reported to date,[4–11] only a few of them possess inherent chirality within their molecular structure.[12] LCs that combine the unique electro-optic characteristics of bent-core molecules with chiral properties are interesting from the view point of molecular design for multifunctional materials. Here we report two new photoresponsive chiral banana-shaped molecules stabilizing exclusively the cholesteric mesophase. Interestingly, selective reflection bands from the N* phase were switchable with changing temperature, light irradiation and an applied electric field. Cholesteric materials with tunable reflection colors are attractive for reflective displays,[13] color reflectors and filters,[14] tunable lasers,[15] molecular sensors[16] and other biomedical applications.[17] Considerable progress has been made in recent years towards reflection color control by changing temperature and light irradiation.[3] However, demonstrations of electrically tunable reflection color have so far been limited to polymer-stabilized cholesteric LC mixtures.[18] In most of these polymer based cholesteric systems, the electrically induced color is not tunable after polymerization of the polymer network. Therefore the novelty of the cholesteric phase reported here lies in its low molecular weight single component molecular system that is truly multifunctional so that the reflection colors are tunable by three different external stimuli, *i.e.* temperature, light and electric field. It has also been reported that doping achiral banana-shaped molecules in chiral host LCs such as cholesteric,[19] SmC* and SmC_A* phases[20] enhances the chirality of the systems. This is in contrary to the generally observed phenomenon that when a chiral system is doped with achiral molecules, the chirality of the initial system gets diluted.[2a] On the other hand, the ability of chiral bent-core molecules to induce chiral mesophases in achiral nematic system has so far not been reported. Therefore, we also investigated for the first time the efficiency of these molecules as a chiral transfer agent in a host nematic LC.

Results and discussion

Synthesis and characterization

The target banana-shaped molecules **1** and **2** with azo (–N=N–) linkage and a chiral centre in the terminal aliphatic chain were synthesized following the general procedure as shown in Scheme 1. Azobenzene moiety incorporated as a linking unit in one of the rigid arms renders photoresponsive property to the molecules.

Liquid Crystal Institute, Kent State University, Kent, Ohio, 44242, USA. E-mail: qli1@kent.edu; Fax: +1-330-672-2796; Tel: +1-330-672-1537

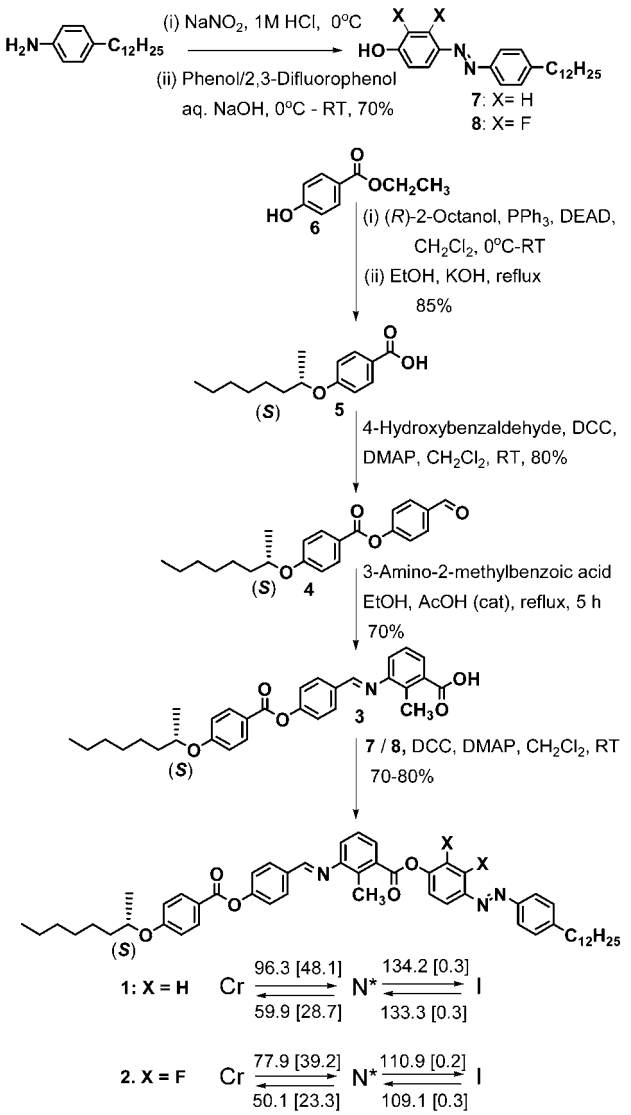

Scheme 1 Synthesis, phase transition temperatures (T/°C) and the corresponding enthalpies [J g^{-1}] of the chiral banana-shaped molecules **1** and **2**. Abbreviations: Cr = crystal, N* = chiral nematic, and I = isotropic.

Isomerization of azobenzene upon irradiation with light is a well-known phenomenon and the possibilities that this reaction offers for the control of liquid crystalline properties have been well-documented.[21] Compound **2** differs from **1** in having lateral fluorine atoms as substituents. Substitution of fluorine atom in LC banana-shaped molecules brings about remarkable modifications to the melting point, transition temperature, mesophase morphology and other physical parameters.[22] The target compounds were purified by column chromatography followed by repeated recrystallizations from ethanol/CH_2Cl_2 solvent mixture. The structure and purity of the compounds were checked by ^{1}H NMR, ^{13}C NMR, high resolution MS and elemental analysis. In order to characterize the absorption properties of the compounds, we carried out UV-Vis spectroscopy measurements in solution. Fig. 1 shows the absorption spectra of **1** (4.5×10^{-5} M) and **2** (4.1×10^{-5} M) in $CHCl_3$ at 298 K and the corresponding changes upon UV (λ_{max} = 365 nm, 6.0

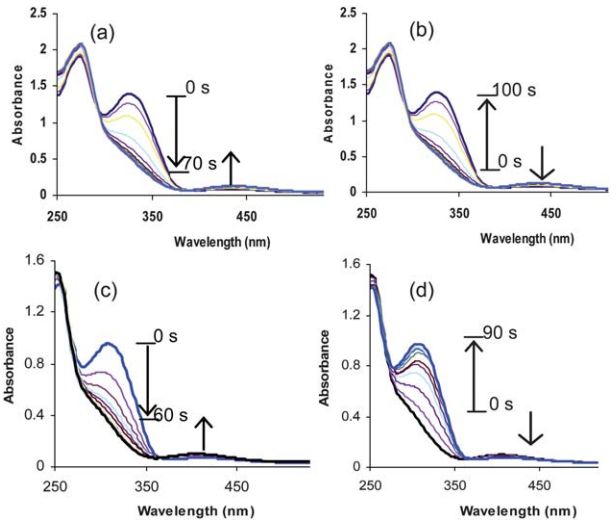

Fig. 1 Photoisomerization of compounds **1** and **2** monitored by UV-Vis spectroscopy: *trans* to *cis* isomerisation by 365 nm irradiation of **1** (a) and **2** (c) and reversible *cis* to *trans* isomerisation by 440 nm irradiation for **1** (b) and **2** (d).

mW cm^{-2}) and visible light (λ_{max} = 440 nm, 2.0 mW cm^{-2}) irradiations.

UV spectrum of the pure *trans* isomer of compound **1** shows two absorption bands between 250 and 500 nm region with maximum absorption at 276 nm (Fig. 1a). Absorption band 300–370 nm (λ_{max} = 326 nm) is related to π–π* transition of the azo chromophore. Upon UV irradiation, due to photochemical *trans* to *cis* isomerization, there is a gradual decrease seen in the absorption maximum of the π–π* transition band with a concomitant increase in the n–π* transition band around 440 nm. Photostationary state (PSS) was reached after UV irradiation for about 70 s. Absorption bands returned to the initial state after several hours in the dark due to the thermal *cis* to *trans* isomerization of the azo moiety. A rapid reversible isomerization was induced by visible light irradiation and a PSS_{Vis} was obtained within 100 s (Fig. 1b). Spectral bands and the isomerization properties of compound **2** were similar to its non-fluorinated analogue **1** except for a 20 nm blue shift seen in its absorption maxima (Fig. 1c and d).

Phase transition behavior of the compounds was investigated by polarizing optical microscopy (POM) and differential scanning calorimetry (DSC). The transition temperatures with the corresponding LC phase assignments are given in Scheme 1. On heating, two endothermic peaks corresponding to the crystal to mesophase and mesophase to isotropic transitions were observed in DSC thermograms for both target compounds. The two corresponding exothermic peaks appear on cooling, indicating the existence of one enantiotropic mesophase. Compared with compound **1**, the lateral fluorine substituted compound **2** exhibits lower transition temperature and a shorter mesophase range. On cooling from the isotropic liquid phase, a typical oily-streak texture characteristic for the cholesteric phase is observed for both compounds. As a representative case, an optical texture observed for compound **2** on cooling from the isotropic phase under planar alignment conditions is shown in Fig. 2 (top). Compared to their corresponding achiral compounds, chiral

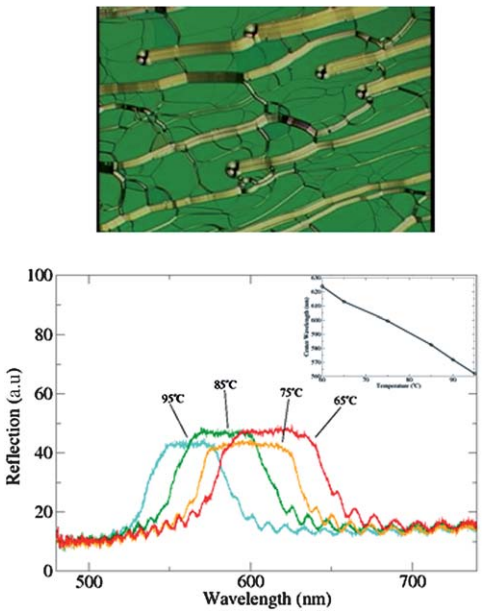

Fig. 2 Crossed polarizing optical photomicrograph of the cholesteric phase of compound **2** on cooling from the isotropic liquid phase at 80 °C (top) and thermally induced change in the selective reflection spectra of compound **2**. The inset shows the red shift of the central wavelength of reflection spectra with decreasing temperature.

derivatives **1** and **2** with branched aliphatic chains show reduced transition temperatures and a complete suppression of the higher ordered smectic phases.[23,24]

Effect of temperature on the reflection colors

Cholesteric phase has a helical structure in which the average direction of molecules rotates around a helical axis. When light propagates through the N* phase with pitch length P, it Bragg reflects light peaked at wavelength $\lambda = n \times P$ with bandwidth $\Delta\lambda = \Delta n \times P$, where n and Δn are the average refractive index and birefringence, respectively.[2a] When the helical pitch is comparable with the wavelengths of visible light, we see reflection colors from the cholesteric phase. Interestingly, the pitch length of the N* phase of compounds **1** and **2** was in the appropriate range to get reflection colors for the entire range of the mesophase. Fig. 2 (bottom) shows the dependence of selective reflection spectra on temperature for compound **2** measured in the cooling cycle. Red shift of the wavelength of the peak reflection with decreasing temperature has been observed for both compounds. Such a behavior is commonly observed in pure calamitic liquid crystals which have the smectic A or smectic C phase at lower temperature. This phenomenon is attributed to the pretransition smectic states (cybotactic clusters) formed in the cholesteric phase.[25] Experimentally it has been observed that small domains with a local smectic organization appear in the nematic phase of banana-shaped molecules at lower temperature close to the phase transition point.[26] Therefore we attribute the temperature dependent changes seen in the reflection wavelength of these materials to the formation of cybotactic clusters. As the cholesteric phase is cooled, the cybotactic clusters become more pronounced leading to an elongation of the cholesteric pitch and a bathochromic shift in the reflection colors.

Effect of light irradiation on the cholesteric reflection colors

The first indication of the influence of light irradiation on the mesomorphic behavior of these molecules was evidenced from the shift in isotropic phase transition temperatures observed under variable light intensity of the microscope lamp. The stronger the illumination, the more the isotropic transition was shifted towards low temperatures. Continuous UV irradiation for few seconds (λ_{max} = 365 nm, 10.0 mW cm^{-2}) onto a planar aligned cholesteric phase in a 5 μm thick cell resulted in an isotropic state isothermally. As soon as the light is removed, the illuminated zone entered back into the mesophase. We observed this phenomenon over the entire range of the cholesteric phase, *i.e.* from 60 °C to 133 °C for compound **1** and from 50 °C to 109 °C for compound **2**. Fig. 3 shows the dependence of the central reflection wavelength of compound **2** upon exposure to a low intensity UV irradiation (λ_{max} = 365 nm, ~5.0 mW cm^{-2}). These changes can be attributed to *trans* to *cis* isomerisation of the azo moiety in the compounds. Formation of small amount of *cis* isomer causes a blue shift in the selective reflection band. A plausible mechanism is that the *cis* isomer of the molecule has a zigzag shape which can disrupt the thermally induced smectic clusters to shorten the helical pitch and hypsochromically shift the reflection band. Upon continuous UV irradiation, the *cis* population increases and completely disrupts the LC ordering to induce cholesteric to isotropic phase transition. Once the UV illumination is off, the *cis* population slowly diminishes and the azo unit returns to the thermodynamically more stable *trans* isomers. This reversible isomerization can occur much faster with visible light irradiation leading to a quick restoration of the mesophase.

On the other hand, a photoinduced shift in cholesteric pitch can also occur due to the difference in twisting ability of the *trans* and *cis* isomers of a molecule.[3] In order to find out if that can be the case, we measured the helical twisting power (HTP) of the *trans* and *cis* isomers of **1** and **2** in a nematic LC host E7. The ability of a chiral dopant to induce a helical pitch is defined as helical twisting power (β) according to the equation: $\beta = 1/PC$, where P and C are the helical pitch length and the concentration of a chiral dopant respectively.[3] Induced chiral nematic phase was directly evidenced as a finger print texture under a POM. We

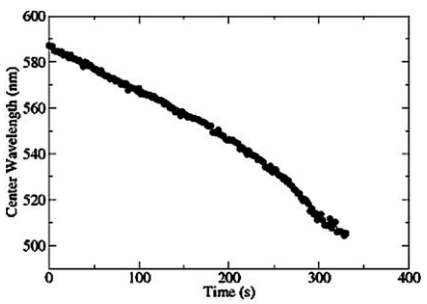

Fig. 3 Change in the central reflection wavelength of the N* phase of compound **2** at 75 °C using continuous UV irradiation (λ_{max} = 365 nm, 5.0 mW cm^{-2}).

measured the induced pitch P by Cano's wedge method.[27] The β value for *trans* isomer of **1** in E7 was found to be 4.5 μm^{-1} while that for compound **2** was about 3.3 μm^{-1}. The low HTP values can be attributed to the conformational flexibility of the banana-shaped molecules and their point chiral nature wherein one chiral carbon center accounts for the chirality of the entire system. Photoinduced changes in HTP of the dopants were directly observed as a change in distance between the Cano lines when sample in a wedge cell was observed with a POM under UV irradiation. A further decrease in β values was observed due to *trans* to *cis* isomerization of the compounds. Since *cis* isomers of these compounds have a lower HTP, a light induced hypsochromic shift seen in the reflection band of the N* phase of the compounds **1** and **2** can be better explained by changes in the ordering of cybotactic clusters.

Effect of electric field on the reflection colors

In order to measure an electric field induced shift of the reflected color, we filled compound **2** into an electro-optical cell (10 μm cell gap) whose inner surfaces were coated with an anti-parallely rubbed polyimide alignment layer (PI-2555). The electro-optic measurements were carried out in the N* phase of the sample at 65 °C. In the absence of any applied voltage, the sample exhibits a reflection maximum around 620 nm. Fig. 4 shows the plot of change in the reflected central wavelength against the applied voltage. Upon the application of a voltage across the cell from 0 to 50 V and 1 kHz frequency, the λ_{max} shifted from 620 nm to 520 nm. The observed blue shift in the reflected wavelength can be explained from the bending of the cholesteric layers. As voltage is applied across the cell, the helix axis tends to tilt to reduce the electric energy, leading to the bending of the layers. The reflection is blue shifted according to the equation below:

$$\lambda = \lambda_0 \cos(\theta)$$

where λ is the central wavelength of the reflection bend, λ_0 is the initial reflection wavelength at 0 V, and θ is the angle between the helix axis and the cell normal. As the tilt takes place, a blue shift is observed. That is the same effect as tilting a cell with a regular cholesteric liquid crystal, where the Bragg reflection is changed with the angle of incidence. A loss in reflectivity with increasing voltage is observed due to the growth of focal conic domains

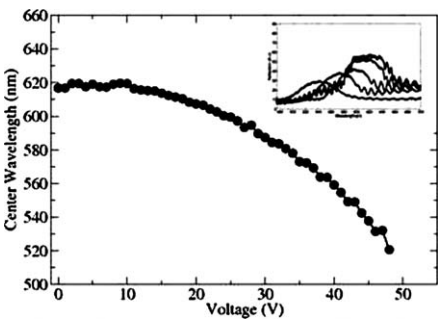

Fig. 4 Center of the reflection wavelength *vs.* voltage in the N* phase of compound **2** at 65 °C. Higher the electrical field, higher is the layer tilt and consequently the blue shift. The inset shows the measured reflection spectra under different voltages.

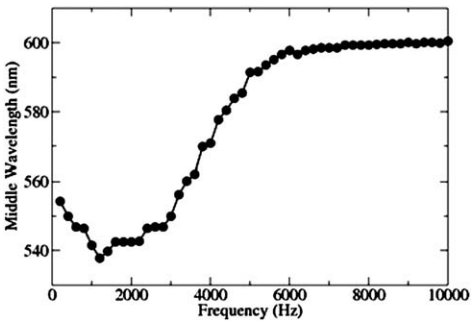

Fig. 5 Peak reflections as a function of frequency under a 40 V electric field applied to the cell.

from the undulations. However, even for high voltage the reflection is not zero and is comparable to other studies when polymer network is used to tune the color or to stabilize the color.[18a,b]

In Fig. 5 we plot the change in the center of the reflection wavelength against the applied frequency when the cell is subjected to a 40 V electric field. The reflection peak does not change (is comparable to the reflection at 0 V) for frequencies higher than 6 kHz. This is because the dielectric anisotropy changes sign and becomes negative around 6 kHz and orient the molecules perpendicular to the applied electric field.[2] As we decrease the frequency, there is a gradual blue shift seen in the reflection peak. This can be attributed to the increase in $\Delta\varepsilon$ as the frequency is decreased. Therefore, the electrical field induced shift becomes more pronounced at lower frequencies since the torque exerted by the field becomes higher. We obtained the maximum shift for an applied frequency of about 1.5 kHz (minimum on the plot). Further study is required to understand the reflection wavelength shift seen for frequencies below 1.5 kHz.

Conclusions

Compounds **1** and **2** reported here are the first examples of chiral bent-core mesogens that stabilize exclusively the N* mesophase over a wide temperature range. Smectic mesophases predominantly seen in bent-core mesogens were completely suppressed in these molecules due to the steric intermolecular interactions arising from unsymmetrical nature of the molecules. The reflection colors from the cholesteric phase were reversibly tunable by external stimuli such as temperature, light and electric field. The mechanism for red shift in reflection band by changing the temperature (upon cooling) or by UV irradiation is postulated on the basis of a cybotactic smectic cluster formed or destroyed in the cholesteric phase. Electric field induced blue shift in reflection band is attributed to the field induced tilting of the cholesteric helix leading to a shortening of the pitch. These findings are of significant importance for the design of new low molecular weight multi-stimuli responsive cholesteric materials with full range tunable reflection colors at ambient temperatures for reflective display applications and for full color recording media. Considering the shape biaxiality of the bent-core molecules and wide range stabilization of the cholesteric mesophase, we see these mesogens as potential candidates for the *hitherto* unknown thermotropic biaxial chiral nematic phase[28] and the characterization studies in this direction are currently in progress.

Experimental section

Instrumentation

All reagents and chemicals were purchased from Aldrich Chemical and were used as received. ^{1}H and ^{13}C NMR spectra were recorded on a Varian Gemini 200. The chemical shifts are reported in δ (ppm) relative to tetramethylsilane as internal standard. Textures and transition temperatures for target compounds were observed by optical microscopy using a Leitz polarizing microscope in conjunction with a Linkam TMS temperature controller. Calorimetric measurements were performed on a Perkin-Elmer differential scanning calorimeter (scanning rate 5 °C min^{-1}). Transition temperatures were taken at the maximum of transition peaks. All UV-Vis spectroscopy experiments were performed on a Perkin-Elmer lambda 19 spectrometer. Photoisomerization was carried out with a Xenon light source (100 W, LAX-cute) through an appropriate filter (365 or 440 nm). Selective reflection spectra measurements were carried out at normal incident of white light illumination and detected from a normal angle by using an Ocean Optics spectrometer. Cholesteric pitch was determined by measuring the intervals of Cano's lines appearing on the surfaces of wedge-type liquid crystalline cells (EHC, KCRK-07, tan $\theta = 0.0194$). The relationship between the distances of Cano's lines and the helical pitch P is $P = 2R \tan \theta$, where R represents the distance between Cano's lines and θ is the angle between the cells. Then helical twisting power (HTP) β is calculated according to the equation: $\beta = (PC)^{-1}$, where P and C are the helical pitch length and the concentration of a chiral dopant expressed in weight fraction (w/w).

General synthetic procedures for compounds 1 and 2

The target compounds **1** and **2** were prepared in a facile synthesis as shown in Scheme 1.[24] Reaction of commercially purchased compound **6** with (*R*)-2-octanol under Mitsunobu reaction conditions followed by base hydrolysis gave the chiral acid derivate compound **5**. We obtained the aldehyde derivative **4** by treating **5** with 4-hydroxybenzaldehyde under the reaction condition of *N*,*N*-dicyclohexyl carbodiimide (DCC) and dimethylaminopyridine (DMAP). Condensation reaction of **4** with 3-amino-2-methylbenzoic acid gave the Schiffs base compound **3**. Diazotization of phenol or 2,3-difluoro phenol with dodecylaniline gave the intermediates **7** or **8** respectively. To a solution of acid compound **3** (1 eq.) in CH_2Cl_2 was added hydroxyazobenzene derivative **7** or **8** (1 eq.), DCC (1.1 eq.) and DMAP (0.01 eq.). The solution was stirred under inert atmosphere for 8 h at room temperature. The reaction mixture was then filtered and the filtrate was washed with 5% aqueous hydrochloric acid, water and then dried over $MgSO_4$. Removal of methylene chloride under reduced pressure gave pale yellow solid. Recrystallisations from EtOH–CH_2Cl_2 solvent mixture (3 times) afforded pure yellowish crystalline compound in 70–80% yield.

Data for 1. ^{1}H NMR ($CDCl_3$): δ 8.37 (s, 1H, –CH=N–), 8.17–7.84 (m, 9H, ArH), 7.41–7.13 (m, 8H, ArH), 6.97 (d, 2H, $J = 8$ Hz, ArH), 4.50 (m, 1H, 1× –CH), 2.69 (m, 5H, Ar–CH_3, 1× Ar–CH_2), 1.69–1.26 (m, 33H, 1× –CH_3, 15× –CH_2), 0.88 (m, 6H, 2× –CH_3). ^{13}C NMR ($CDCl_3$): 165.8, 164.6, 163.0, 159.4, 153.7, 152.7, 152.5, 150.9, 150.4, 146.7, 134.6, 133.7, 132.4, 130.1, 129.8, 129.1, 128.0, 126.4, 124.0, 122.9, 122.4, 120.8, 115.3, 74.2, 36.3, 35.9, 31.9, 31.8, 31.3, 29.6, 29.5, 29.4, 29.3, 29.2, 29.1, 25.4, 22.7, 22.6, 19.6, 15.4, 14.1. HRMS: *m*/*z* calcd for $C_{54}H_{66}N_3O_5$ (M + H): 836.5002. Found: 836.5034. Elemental analysis calcd for $C_{54}H_{65}N_3O_5$: C 77.57, H 7.84, N 5.03%. Found: C 76.98, H 7.85, N 5.02%.

Data for 2. ^{1}H NMR ($CDCl_3$): δ 8.34 (s, 1H, CH=N–), 8.18–7.88 (m, 7H, ArH), 7.50 (d, 1H, $J = 7$ Hz, ArH), 7.37–7.12 (m, 7H, ArH), 6.97 (d, 2H, $J = 8$ Hz, ArH), 4.50 (m, 1H, 1× –CH), 2.69 (m, 5H, Ar–CH_3, 1× Ar–CH_2), 1.66–1.27 (m, 33H, 1× –CH_3, 15× –CH_2), 0.89 (m, 6H, 2× –CH_3). ^{13}C NMR ($CDCl_3$): 164.6, 164.3, 163.0, 159.5, 153.8, 152.6, 151.9, 150.9, 147.8, 146.7, 141.3, 139.8, 135.1, 133.6, 132.4, 130.1, 129.2, 128.6, 128.3, 126.5, 123.4, 122.8, 122.4, 120.8, 118.3, 115.3, 111.9, 74.2, 36.3, 36.0, 31.9, 31.8, 31.2, 29.7, 29.6, 29.5, 29.3, 29.2, 29.1, 25.4, 22.7, 22.6, 19.6, 15.3, 14.1. HRMS: *m*/*z* calcd for $C_{54}H_{64}F_2N_3O_5$ (M + H): 872.4814. Found: 872.4853. Elemental analysis calcd for $C_{54}H_{63}F_2N_3O_5$: C 74.37, H 7.28, F 4.36, N 4.82%. Found: C 74.12, H 7.49, F 4.62, N 4.86%.

Acknowledgements

The work is supported by the Department of Energy (DOE DE-SC0001412), the Air Force Office of Scientific Research (AFOSR FA9550-09-1-0193), and the National Science Foundation (NSF IIP 0750379).

References

1 (*a*) *Supramolecular Chirality*, ed. M. Crego-Calama and D. N. Reinhoudt, Springer, Berlin, 2006; (*b*) *Molecular Devices and Machines: A Journey into the Nanoworld*, ed. V. Balzani, M. Venturi and A. Credi, Wiley-VCH, Weinheim, 2003; (*c*) *Molecular Switches*, ed. B. L. Feringa, Wiley-VCH, Weinheim, 2001; (*d*) K. Kinbara and T. Aida, *Chem. Rev.*, 2005, **105**, 1377–1400.

2 (*a*) *The Physics of Liquid Crystals*, ed. P. G. de Gennes and J. Prost, Clarendon, Oxford, 2nd edn, 1993; (*b*) *Handbook of Liquid Crystals: Vol. 1. Fundamentals*, ed. D. Demus, J. Goodby, G. W. Gray, H.-W. Spiess and V. Vill, Wiley-VCH, Weinheim, 1998; (*c*) *Chirality in Liquid Crystals*, ed. H.-S. Kitzerov and C. Bahr, Springer, New York, 2001; (*d*) *Ferroelectric and Antiferroelectric Liquid Crystals*, ed. S. T. Lagerwall, Wiley-VCH, Weinheim, 2000.

3 (*a*) R. Eelkema and B. L. Feringa, *Org. Biomol. Chem.*, 2006, **4**, 3729–3745; (*b*) C. J. Boulton, J. G. Finden, E. Yuh, J. J. Sutherland, M. D. Wand, G. Wu and R. P. Lemieux, *J. Am. Chem. Soc.*, 2005, **127**, 13656–13665; (*c*) Q. Li, L. Green, N. Venkataraman, I. Shiyanovskaya, A. Khan, A. Urbas and J. W. Doane, *J. Am. Chem. Soc.*, 2007, **129**, 12908–12909; (*d*) L. Green, Y. Li, T. White, A. Urbas, T. Bunning and Q. Li, *Org. Biomol. Chem.*, 2009, **7**, 3930–3933; (*e*) T. J. White, R. L. Bricker, L. V. Natarajan, N. V. Tabiryan, Q. Li and T. J. Bunning, *Adv. Funct. Mater.*, 2009, **19**, 3484–3488; (*f*) J. Ma, Y. Li, T. J. White, A. Urbas and Q. Li, *Chem. Commun.*, 2010, **46**, 3463–3465; (*g*) M. Mathews and N. Tamaoki, *J. Am. Chem. Soc.*, 2008, **130**, 11409–11416; (*h*) M. Kawamoto, T. Aoki, N. Shiga and T. Wada, *Chem. Mater.*, 2009, **21**, 564–572; (*i*) S. Pieraccini, S. Masiero, A. Ferrarini and G. P. Spada, *Chem. Soc. Rev.*, 2010, DOI: 10.1039/b924962.

4 (*a*) T. Niori, T. Sekine, J. Watanabe, T. Furukawa and H. Takezoe, *J. Mater. Chem.*, 1996, **6**, 1231–1233; (*b*) R. Amaranatha Reddy and C. Tschierske, *J. Mater. Chem.*, 2006, **16**, 907–961.

5 (*a*) D. M. Walba, E. Korblova, R. Shao, J. E. Macelennan, D. R. Link, M. A. Glaser and N. A. Clark, *Science*, 2000, **288**, 2181–2184; (*b*) S. W. Choi, S. Kang, Y. Takanishi, K. Ishikawa, J. Watanabe and H. Takezoe, *Chirality*, 2007, **19**, 250–254.

6 H. Takezoe and Y. Takanishi, *Jpn. J. Appl. Phys.*, 2006, **45**, 597–625.

7 K. Shiromo, D. A. Sahade, T. Oda, T. Nihira, Y. Takanishi, K. Ishikawa and H. Takezoe, *Angew. Chem., Int. Ed.*, 2005, **44**, 1948–1951.
8 S. W. Choi, S. Kang, Y. Takanishi, K. Ishikawa, J. Watanabe and H. Takezoe, *Angew. Chem., Int. Ed.*, 2006, **45**, 6503–6506.
9 S. W. Choi, T. Izumi, Y. Hoshino, Y. Takanishi, K. Ishikawa, J. Watanabe and H. Takezoe, *Angew. Chem., Int. Ed.*, 2006, **45**, 1382–1385.
10 L. E. Hough and N. A. Clark, *Phys. Rev. Lett.*, 2005, **95**, 107802-1–107802-4.
11 F. Araoka, N. Y. Ha, Y. Kinoshita, B. Park, J. W. Wu and H. Takezoe, *Phys. Rev. Lett.*, 2005, **95**, 137801-1–137801-4.
12 (*a*) M. Nakata, D. R. Link, F. Araoka, J. Thisayukta, Y. Takanishi, K. Ishikawa, J. Watanabe and H. Takezoe, *Liq. Cryst.*, 2001, **28**, 1301–1308; (*b*) G. Gesekus, I. Dierking, S. Gerber, M. Wulf and V. Vill, *Liq. Cryst.*, 2004, **31**, 145–152; (*c*) R. A. Reddy, B. K. Sadashiva and U. Baumeister, *J. Mater. Chem.*, 2005, **15**, 3303–3316.
13 (*a*) *Reflective Liquid Crystal Displays*, ed. S.-T. Wu and D.-K. Yang, Wiley, Chichester, 2001; (*b*) D.-K. Yang, J. L. West, L.-C. Chien and J. W. Doane, *J. Appl. Phys.*, 1994, **76**, 1331–1333; (*c*) N. Venkataraman, G. Magyar, E. Montbach, A. Khan, T. Schneider, J. W. Doane, L. Green and Q. Li, *J. Soc. Inf. Disp.*, 2009, **17**, 869–873.
14 (*a*) N. A. Ha, Y. Ohtsuka, S. M. Jeong, S. Nishimura, G. Suzaki, Y. Takanishi, K. Ishikawa and H. Takezoe, *Nat. Mater.*, 2008, **7**, 43–47; (*b*) M. Mitov and N. Dessaud, *Nat. Mater.*, 2006, **5**, 361–364; (*c*) J. Lub, P. van de Witte, C. Doornkamp, J. P. A. Vogels and R. T. Wegh, *Adv. Mater.*, 2003, **15**, 1420–1425; (*d*) A. Hochbaum, Y. Jiang, L. Li, S. Vartak and S. Faris, *SID Digest*, 1999, **30**, 1063–1065.
15 (*a*) V. I. Kopp, B. Fan, H. K. M. Vithana and A. Z. Genack, *Opt. Lett.*, 1998, **23**, 1707–1709; (*b*) S. Furumi and N. Tamaoki, *Adv. Mater.*, 2010, **22**, 886–891.
16 P. Raynes, S. J. Cowling and J. W. Goodby, *Anal. Methods*, 2009, **1**, 88–92.
17 (*a*) *Liquid Crystals: Frontiers in Biomedical Applications*, ed. S. J. Woltman, G. D. Jay and G. P. Crawford, World Scientific, 2007; (*c*) G. T. Stewart, *Liq. Cryst.*, 2003, **30**, 541–557; (*c*) J. Hoogboom, J. Clerx, M. B. J. Otten, A. E. Rowan, T. Rasing and R. J. M. Nolte, *Chem. Commun.*, 2003, 2856–2857; (*d*) S. J. Woltman, G. D. Jay and G. P. Crawford, *Nat. Mater.*, 2007, **6**, 929–938.
18 (*a*) H. Xianyu, T.-H. Lin and S.-T. Wu, *Appl. Phys. Lett.*, 2006, **89**, 091124; (*b*) S.-Y. Lu and L.-C. Chien, *Appl. Phys. Lett.*, 2007, **91**, 131119; (*c*) J. Chen, S. M. Morris, D. T. Wilkinson and H. T. Coles, *Appl. Phys. Lett.*, 2007, **91**, 121118; (*d*) A. Bobrovsky and V. Shibaev, *J. Mater. Chem.*, 2009, **19**, 366–372.
19 (*a*) J. Thisayukta, H. Niwano, H. Takezoe and J. Watanabe, *J. Am. Chem. Soc.*, 2002, **124**, 3354–3358; (*b*) M. Nakata, Y. Takanishi, J. Watanabe and H. Takezoe, *Phys. Rev. E: Stat., Nonlinear, Soft Matter Phys.*, 2003, **68**, 041710-1–041710-6.
20 E. Gorecka, M. Cepic, J. Mieczkowski, M. Nakata, H. Takezoe and B. Zeks, *Phys. Rev. E: Stat., Nonlinear, Soft Matter Phys.*, 2003, **67**, 061704-1–061704-4.
21 (*a*) K. Ichimura, *Chem. Rev.*, 2000, **100**, 1847–1873; (*b*) V. A. Mallia and N. Tamaoki, *Chem. Soc. Rev.*, 2004, **33**, 76–84.
22 M. Hird, *Chem. Soc. Rev.*, 2007, **36**, 2070–2095.
23 V. Prasad, S.-W. Kang, K. A. Suresh, L. Joshi, Q. Wang and S. Kumar, *J. Am. Chem. Soc.*, 2005, **127**, 17224–17227.
24 M. Mathews, S.-W. Kang, S. Kumar and Q. Li, *Liq. Cryst.*, 2010, DOI: 10.1080/02678292.2010.524716.
25 (*a*) F. Zhang and D.-K. Yang, *Liq. Cryst.*, 2002, **29**, 1497–1501; (*b*) V. A. Mallia and N. Tamaoki, *J. Mater. Chem.*, 2003, **13**, 219–224.
26 (*a*) O. Francescangeli, V. Stanic, S. I. Torgova, A. Strigazzi, N. Scaramuzza, C. Ferrero, I. P. Dolbnya, T. M. Weiss, R. Berardi, L. Muccioli, S. Orlandi and C. Zannoni, *Adv. Funct. Mater.*, 2009, **19**, 1–9; (*b*) W. Weissflog, S. Sokolowski, H. Dehne, B. Das, S. Grande, M. W. Schroder, A. Eremin, S. Diele, G. Pelzl and H. Kresse, *Liq. Cryst.*, 2004, **31**, 923–933.
27 *Textures of Liquid crystals*, ed. I. Dierking, Wiley-VCH, Weinheim, 2003.
28 T. Kroin, A. M. F. Neto, L. Liebert and Y. Galerne, *Phys. Rev. A: At., Mol., Opt. Phys.*, 1989, **40**, 4647–4651.